Geophysical Journal International

Geophys. J. Int. (2017) **209,** 661–671 doi: 10.1093/gji/ggx045
Advance Access publication 2017 February 2
GJI Seismology

A physical solution for plane *SH* waves in anelastic media

Bjorn Ursin,[1,2] José M. Carcione[3] and Davide Gei[3]

[1]*Centro de Pesquisa em Geofísica e Geologia (CPPG/UFBA) and National Institute of Science and Technology of Petroleum Geophysics (INCT-GP/CNPQ), Instituto de Geociências, Universidade Federal da Bahia, Campus Universitário da Federação, Salvador, Bahia, Brazil*
[2]*The Norwegian University of Science and Technology (NTNU), Department of Geoscience and Petroleum, S. P. Andersensvei 15A, NO-7491 Trondheim, Norway*
[3]*Istituto Nazionale di Oceanografia e di Geofisica Sperimentale (OGS), Borgo Grotta Gigante 42c, I-34010 Sgonico, Trieste, Italy. E-mail: jcarcione@inogs.it*

Accepted 2017 February 1. Received 2017 January 31; in original form 2016 June 15

SUMMARY

In a lossy medium with complex frequency-dependent wave speed both rays and plane waves at an interface should satisfy the dispersion relation (that is, the wave equation), the radiation condition (the amplitude should go to zero at infinity) and the horizontal complex slowness should be continuous (Snell's law). It is known that this may lead to a transmitted wave which violates the radiation condition and which also causes problems with the phase of the reflection coefficient. In fact, ray-tracing algorithms and analytical evaluations of the reflection and transmission coefficients in anelastic media may lead to non-physical solutions related to the complex square roots of the vertical slowness and polarizations. The steepest-descent approximation with complex horizontal slowness involves non-physical complex horizontal distances, and in some cases also a non-physical vertical slowness that violates the radiation condition. Similarly, the reflection and transmission coefficients and ray-tracing codes obtained with this approach yields wrong results. In order to tackle this problem, we choose the stationary-phase approximation with real horizontal slowness. This gives real horizontal distances, the radiation condition is always satisfied and the reflection and transmission coefficients are correct. This is shown by comparison to full-wave space-time modelling results by computing the reflection and transmission coefficients and respective phase angles from synthetic seismograms. This numerical evaluation is based on a 2-D wavenumber-frequency Fourier transform. The results indicate that the stationary-phase method with a real horizontal slowness provides the correct physical solution.

Key words: Body waves; Seismic anisotropy; Seismic attenuation; Theoretical seismology; Wave propagation; Acoustic properties.

1 INTRODUCTION

Wave propagation in lossy media involves a number of unclear issues concerning the definition of energy (e.g. Carcione 1999), the Snell–Fermat equivalence (Carcione & Ursin 2016) and the correct calculation of the reflection and transmission coefficients (Krebes & Daley 2007). Regarding the last issue, the problem of effectively tracing seismic rays and evaluating the corresponding reflection coefficients in attenuating media is due to the ambiguities related to the signs of the complex-valued square roots involved in the expression of the vertical slownesses, which result in a set of mathematically correct but non-physical solutions (Richards 1984; Krebes & Daley 2007).

Both for rays and plane waves, the solution should satisfy:

(1) The dispersion relation (that is, the wave equation).
(2) The radiation condition (the amplitude should go to zero at infinity).
(3) The horizontal complex slowness (in the tangential plane at an interface for reflected and transmitted waves) should be continuous.

Vavryčuk (2008, 2010) has improved the theory of ray tracing in anelastic media by introducing energy-based quantities. The equations, which hold for smoothly inhomogeneous anisotropic low-loss viscoelastic media, are based on real-valued rays defined as trajectories based on an inhomogeneous complex and stationary slowness vector, where by inhomogeneous we mean a plane wave whose propagation and attenuation directions are not the same. The problem of the vertical slowness is solved by invoking the radiation condition and the concept of critical angle, but as Krebes & Daley (2007) show, imposing the radiation condition may introduce large errors in the reflection coefficient when the horizontal slowness is complex and the fact that critical angles do not exist in anelastic media (Borcherdt 1977; Carcione 2014) invalidates such a concept as a useful criterion. In our case only the real part of the horizontal slowness is required to be continuous since the imaginary part is nil. The full-wave solution is an integral over the real horizontal slowness. The vertical slowness is complex, given by the dispersion relation, which in our form relates the complex slowness vector to the inverse of the complex velocity squared. The wave is homogeneous only for elastic media and pre-critical waves.

The calculation of the plane-wave displacement reflection and transmission coefficients requires the proper signs of the vertical slownesses of all the events. Generally, a wrong choice yields coefficients varying discontinuously as a function of the angle of incidence. Richards (1984), Krebes & Daley (2007) and Sidler *et al.* (2008) have analysed this problem for a homogeneous wave incident on a plane interface. Richards (1984) showed that for a homogeneous incoming plane wave, the transmitted plane waves may have a vertical slowness corresponding to propagation and attenuation in opposite vertical directions. The outgoing wave is thus violating the radiation condition with increasing amplitude away from the interface. This situation also creates problems with the reflected wave, as the vertical slowness for the transmitted wave is used in computing the reflection coefficient. Krebes & Daley (2007) have shown that this may produce errors in both amplitude and phase of the reflection coefficient. They discuss three choices for the vertical slowness: (i) Propagation away from the interface with increasing amplitude. This was recommended by Richards (1984) and Brokešová & Červený (2002), but it violates the radiation condition, although the first author showed that somehow the violation could be reconciled with the radiation condition. An example shows that there may be phase problems with the reflection coefficient. (ii) Choose the wave which is attenuated away from the interface. However, this wave propagates towards the interface. There is also a discontinuity in the vertical slowness, s_z, when $\mathrm{Im}\left(s_z^2\right)$ becomes negative. They report problems with the reflection coefficient also in this case. (iii) They propose to use the complex conjugate of the vertical slowness when its imaginary part becomes negative. This produces a wave which propagates and is attenuated away from the interface (Daley & Krebes 2015), but it no longer satisfies the dispersion relation (eq. 1). From this discussion, it follows that none of the proposed solutions behave according to accepted physical laws. Krebes & Daley (2007) also compute the stationary-phase solution of the exact slowness integral, and show that this real stationary value of horizontal slowness gives reasonable values for the reflection coefficient. Their approximate solution for the horizontal slowness is the real part of the complex horizontal slowness obtained with the steepest-descent method (eq. 33 is expression to solve for the real horizontal slowness). They used the real part of the complex saddle-point s_x to compute the reflection coefficient, but their traveltime is still that of a homogeneous plane wave.

Sidler *et al.* (2008) use an accurate numerical technique, based on a frequency–slowness approach, to evaluate the plane-wave reflection coefficients in anelastic media. This reference solution is compared to the analytical results based on the vertical slowness component. Sidler *et al.* (2008) explore the analytical solution space and its ambiguities by analysing the paths along the Riemann surfaces associated with the square roots involved in the vertical slowness. This analysis generally provides the correct sign. However, there are some cases that require an alternative solution, because the correct integration path for the vertical slowness does not exist on the corresponding Riemann surface. The approach is essentially equivalent to enforcing continuity of the vertical slowness in the pre-critical range and honouring the radiation condition in the post-critical range.

Daley & Krebes (2004) analyse the slowness integral for a reflected or transmitted *SH* wave at a plane interface between two anelastic isotropic media. They deform the integration path in the complex plane and use the method of steepest descent to compute a stationary value of the vertical slowness which is complex (see also Ruud 2006). This also leads to complex values for the distances between the source and the transmission point and the transmission point and the receiver (denoted complex rays). But the sum is real, equal to the physical horizontal distance between the source and receiver. The problem with the vertical slowness occurs when the product of the real and imaginary parts is negative. Then both the up-going and down-going waves violate the radiation condition. This problem cannot occur when the horizontal slowness is real.

Another issue related to the sign of the vertical slowness is the problem of the 'opposite phase', where the phase shifts predicted by the elastic model are abrupt at the elastic critical angle and opposite in sign from those for an anelastic model. The fact is that this occurs even for a small (negligible) amounts of attenuation. This problem is indicated in Hearn & Krebes (1990), where they obtain a polarity reversal at large offsets (see the fourth trace of their fig. 11), whereas if one uses full-wave theory to compute the same reflected waveform, one does not obtain such a polarity reversal. See page 206 (second paragraph) of Krebes & Daley (2007), where they already show that 'In fact, if exact synthetic seismograms are computed for their example by numerically evaluating the full wavefield integral over *p* (the 'generalized ray'), one finds no polarity reversal between the elastic and anelastic cases'. For more details on this non-physical discrepancy see also figs 3 and 4 in the same paper, which compare the elastic and anelastic cases (first arrival at 1.5 km).

The reflected and transmitted *SH* waves are exactly represented by integrals over real horizontal slowness (Ursin & Stovas 2002). The steepest-descent approximation leads to a non-physical solution with complex horizontal slowness, complex horizontal distances, and a plane-wave solution which possibly violates the radiation condition. We choose the stationary-phase approximation to the slowness integral (Tsvankin 1995). Here, the horizontal slowness and all the horizontal distances are real, and the radiation condition is always satisfied.

Here, we consider the case of *SH*-waves in isotropic media but the mathematical problem is equivalent to those of *P* waves (the acoustic wave equation) and electromagnetic waves, by virtue of the acoustic-electromagnetic analogy (Carcione & Robinson 2002). Moreover, the generalization to the anisotropic case (for *SH* waves) straightforward.

2 PLANE-WAVE INTEGRAL FOR REFLECTED/TRANSMITTED *SH* WAVES

We consider a source and receivers as shown in Fig. 1, where the quantities of the lower medium are primed. The source is located at the horizontal distance x_1 from an unknown reflection/transmission point. Only $x = x_1 + x_2$, z_1, z_2, $x' = x_1 + x_2'$ and z_2' are known. We want to compute x_1 and x_2 (x_2') and the traveltimes for a reflected/transmitted *SH* wave (Krebes & Daley 2007).

The horizontal slowness s_x and the vertical slownesses s_z for the incoming and reflected waves are related by the dispersion relation, which for an isotropic anelastic medium is

$$\mathbf{s} \cdot \mathbf{s} = s_x^2 + s_z^2 = \frac{1}{v^2}, \tag{1}$$

(e.g. Carcione 2014), where v is the complex velocity. Here the complex slowness is

$$\mathbf{s} = \mathbf{s}_R + \mathrm{i}\mathbf{s}_I = (s_x, s_z)^\top = (s_{xR} + \mathrm{i}s_{xI}, s_{zR} + \mathrm{i}s_{zI})^\top. \tag{2}$$

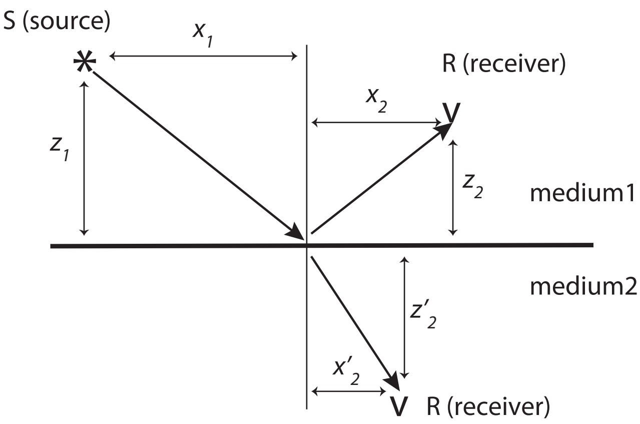

Figure 1. Reflection-transmission problem.

where $i = \sqrt{-1}$ and the subindices '*R*' and '*I*' denote real and imaginary parts, respectively. In eq. (1), the complex velocity satisfies

$$v^2 = v_0^2 \left(1 - \frac{i}{Q}\right) \tag{3}$$

or

$$\frac{1}{v^2} = \frac{1}{v_0^2}\left(\frac{1 + i/Q}{1 + 1/Q^2}\right), \tag{4}$$

where v_0 and Q are the real velocity and quality factor, respectively (Aki & Richards 2002). In the preceding expressions $v_0 = v_h$ for $Q \gg 1$, where v_h is the speed of homogeneous plane waves (for smaller Q, they are not the same).

The vertical slowness s'_z for the transmitted wave is computed from

$$s_x^2 + s_z'^2 = \frac{1}{v'^2}, \tag{5}$$

where v' is the velocity of the lower medium (defined as in eqs 3 and 4).

The scalar displacement of the transmitted wave can be expressed by (Aki & Richards 2002)

$$u(\omega) = \frac{A(\omega)}{4\pi\mu(\omega)} \int \frac{1}{s_z(s_x, \omega)} F(\omega, s_x) \exp[i\omega\tau(\omega, s_x)] ds_x. \tag{6}$$

Here τ is time, ω is the angular frequency, $A(\omega)$ is the source spectrum,

$$\mu(\omega) = \rho v^2 = \rho v_0^2 \left(1 - \frac{i}{Q}\right) = \mu_0 \left(1 - \frac{i}{Q}\right) \tag{7}$$

is the shear modulus (ρ is the mass density), and

$$\tau(\omega, s_x) = \begin{cases} s_x x + s_z z, & \text{for reflection} \\ s_x x' + s_z z_1 + s'_z z'_2, & \text{for transmission} \end{cases} \tag{8}$$

is a complex exponent (with $z = z_1 + z_2$). With the sign convention in eq. (6), positive real and imaginary parts of s_x and s_z correspond to waves propagating and being attenuated in the $+x$ and $+z$ directions, respectively. A schematic of the steepest descent (saddle point) contour for the integral (6) is given in fig. 2 of Daley & Krebes (2004).

The boundary conditions (Snell law) require that s_x is the same for incident and transmitted/reflected plane waves (Richards 1984; Borcherdt & Wennerberg 1985; Borcherdt *et al.* 1986; Hearn & Krebes 1990; Borcherdt 2009; Carcione 2014).

Traveltimes are obtained as $\mathrm{Re}(\tau) = \tau_R$ (e.g. Krebes & Slawinski 1991; Daley & Krebes 2004). In eq. (6), the amplitude function is

$$F(\omega, s_x) = \begin{cases} R = \dfrac{\mu s_z - \mu' s'_z}{\mu s_z + \mu' s'_z}, & \text{for reflection} \\ T = \dfrac{2\mu s_z}{\mu s_z + \mu' s'_z}, & \text{for transmission} \end{cases} \tag{9}$$

(e.g. Carcione 2014). These are actually the reflection and transmission coefficients, since rigorously there are some extra factors (see, for example, Aki & Richards 2002, eq. 6.18, for the *P*-wave case and Krebes & Daley 2007, eq. 9).

In the following, we shall consider only one frequency, ω, and omit this dependence. In eq. (6), the horizontal slowness is complex. However, an exact solution for the displacement is obtained from (Aki & Richards 2002; Chapman 2004)

$$u(\omega) = \frac{A(\omega)}{4\pi\mu(\omega)} \int_{-\infty}^{\infty} \frac{1}{s_z(s_{xR})} F(\omega, s_{xR}) \exp[i\omega\tau(s_{xR})] ds_{xR}, \tag{10}$$

where $s_x = s_{xR}$ is real. Eq. (10) is the integral (6) but with the integration path along the real axis.

3 THE STEEPEST-DESCENT APPROXIMATION

Following Daley & Krebes (2004) we deform the integration path in eq. (10) into the complex plane. The result is an integral like (6) which is evaluated by the method the steepest descent. The complex stationary point, $\bar{s}_x$, is found by solving

$$\frac{\partial\tau}{\partial s_x} = \begin{cases} x + z\dfrac{\partial s_z}{\partial s_x} = 0, & \text{for reflection} \\ x' + z_1 \dfrac{\partial s_z}{\partial s_x} + z'_2 \dfrac{\partial s'_z}{\partial s_x} = 0, & \text{for transmission} \end{cases}. \tag{11}$$

From the dispersion relation (1) we obtain

$$\frac{\partial s_z}{\partial s_x} = -\frac{s_x}{s_z} \tag{12}$$

and a similar equation for the lower medium. Substitution of these expressions into eq. (11) gives for the transmitted wave

$$x' = s_x \left(\frac{z_1}{s_z} + \frac{z'_2}{s'_z}\right). \tag{13}$$

This equation must be solved iteratively for the complex value of s_x, the horizontal slowness of the incoming and transmitted wave, using the dispersion relation (1).

For the reflected wave, the stationarity condition (11), with (12), becomes

$$x = z\frac{s_x}{s_z}. \tag{14}$$

Combining this equation with the dispersion relation (1) gives the stationary values

$$s_x = \frac{x}{rv} = \frac{\sin\psi}{v}, \quad s_z = \frac{z}{rv} = \frac{\cos\psi}{v} \tag{15}$$

where $r = \sqrt{x^2 + z^2}$ and ψ is the angle that the stationary ray makes with the vertical axis. The slowness vector is then

$$\mathbf{s} = \frac{1}{v}(\sin\psi, \cos\psi)^\top. \tag{16}$$

From these equations it follows that the stationary reflected ray is homogeneous, that is, the real and imaginary parts of **s** are parallel (Carcione 2014).

For the reflected wave, the vertical slowness in the lower medium is

$$s_z'^2 = \frac{1}{v'^2} - s_x^2 = \frac{1}{v'^2} - \frac{1}{v^2}\left(\frac{x}{r}\right)^2, \tag{17}$$

where eq. (15) has been used. Note that this is not the vertical slowness for the stationary transmitted wave which must be found using the stationary value of the horizontal slowness, being the solution of eq. (13). In fact, the stationary horizontal slowness components (obeying Snell law) for the reflected and transmitted wave are different, that is, when computing the reflection coefficients the component corresponds to a receiver above the interface (the reflection ray), while the transmission coefficient involves a receiver below the interface (the transmission ray).

For the transmitted wave we must find the complex, stationary values of x_1 and x_2' such that $x' = x_1 + x_2'$ is real. We have

$$x_1 = \frac{s_x}{s_z} z_1, \quad \text{and} \quad x_2' = \frac{s_x}{s_z'} z_2' = x' - x_1. \tag{18}$$

As for eqs (14) and (15), we obtain the complex Snell law

$$s_x = \frac{x_1}{r_1 v} = \frac{x' - x_1}{r_2' v_2'}, \tag{19}$$

where $r_1 = \sqrt{x_1^2 + z_1^2}$ and $r_2' = \sqrt{(x' - x_1)^2 + z_2'^2}$. Eq. (19) must be solved for the complex value of x_1. Alternatively, we may square this equation, giving a fourth-order equation for x_1, see eq. (49).

The steepest-descent approximation for the displacement is now obtained from eq. (6) (Aki & Richards 2002, Box 6.3),

$$u = \frac{A}{4\pi\mu} F(\bar{s}_x) \left| \frac{2\pi}{\omega\tau''(\bar{s}_x)} \right|^{1/2} \frac{\exp[i\omega\tau(\bar{s}_x)]\exp[i\chi(\bar{s}_x)]}{s_z(\bar{s}_x)}. \tag{20}$$

Here

$$\tau'' = \frac{\partial^2\tau}{\partial s_x^2} = \begin{cases} z\dfrac{\partial^2 s_z}{\partial s_x^2}, & \text{for reflection} \\[2ex] z_1\dfrac{\partial^2 s_z}{\partial s_x^2} + z_2'\dfrac{\partial^2 s_z'}{\partial s_x^2}, & \text{for transmission,} \end{cases} \tag{21}$$

where, from the dispersion relation (1),

$$\frac{\partial^2 s_z}{\partial s_x^2} = -\frac{1}{s_z^3 v^2}, \tag{22}$$

with $\tau'' = |\tau''|\exp(i\theta)$, $i\tau'' = |\tau''|\exp[i(\theta + \pi/2)]$, and

$$\chi = -(\theta + \pi/2)/2 \pm \pi/2. \tag{23}$$

The two solutions differ in sign.

4 THE VERTICAL-SLOWNESS PROBLEM

With the sign convention in eq. (6), it is seen that s_{zR} and s_{zI} should have the same sign for a wave to propagate and being attenuated in the same vertical direction. From the dispersion relation (1) we have

$$\mathrm{Im}\left(s_z^2\right) = 2 s_{zR} s_{zI} = \mathrm{Im}\left(\frac{1}{v^2} - s_x^2\right). \tag{24}$$

This quantity should therefore be positive, and for s_x real this is always the case (see eq. 4).

For horizontal slowness s_x complex there will be problems when

$$\mathrm{Im}\left(\frac{1}{v^2} - s_x^2\right) < 0, \tag{25}$$

because then s_{zR} and s_{zI} have opposite sign according to eq. (24). This means that the two plane waves represented by the dispersion relation will propagate and attenuate in opposite directions. That is, both waves violate the radiation condition with respect to their direction of propagation. For the reflected wave this will give problems with the reflection coefficient, involving the vertical slowness in the lower medium (see eq. 17), when

$$\mathrm{Im}\left(\frac{1}{v'^2}\right) < \mathrm{Im}\left(\frac{1}{v^2}\right)\left(\frac{x}{r}\right)^2 \quad \text{or}$$
$$\frac{1}{v_0'^2}\frac{1}{Q' + Q'^{-1}} < \frac{1}{v_0^2}\frac{1}{Q + Q^{-1}}\left(\frac{x}{r}\right)^2. \tag{26}$$

For large values of Q (weak loss) this becomes

$$\frac{1}{v_0'\sqrt{Q'}} < \frac{1}{v_0\sqrt{Q}}\frac{x}{r}. \tag{27}$$

See eq. (28) in Krebes & Daley (2007). They discuss three choices for the vertical slowness, but the problems persist.

The steepest-descent solution with complex horizontal slowness involves non-physical complex horizontal distances, and in some cases also a non-physical vertical slowness that violates the radiation condition. In order to have a solution which is always physical, we choose the stationary-phase solution (e.g. Tsvankin 1995) with a real horizontal slowness, as illustrated in the next section.

5 THE STATIONARY-PHASE SOLUTION

The problems encountered in the previous section can be avoided by approximating the slowness integral (10) by the method of stationary phase (Tsvankin 1995). With $s_{xR} = s_x$, this integral may be written as

$$u = \frac{A}{4\pi\mu}\int_{-\infty}^{\infty}\frac{1}{s_z(s_x)}F(s_x)\exp[i\omega\tau_R(s_x) - \omega\tau_I(s_x)]\mathrm{d}s_x. \tag{28}$$

The stationarity conditions are

$$\frac{\partial\tau_R}{\partial s_x} = \begin{cases} x + z\dfrac{\partial s_{zR}}{\partial s_x} = 0, & \text{for reflection} \\[2ex] x' + z_1\dfrac{\partial s_{zR}}{\partial s_x} + z_2'\dfrac{\partial s_{zR}'}{\partial s_x} = 0, & \text{for transmission} \end{cases} \tag{29}$$

From the dispersion relation (1) we obtain for the upper medium

$$\frac{\partial s_{zR}}{\partial s_x} = -\frac{s_x s_{zR}}{|s_z|^2} \tag{30}$$

and a similar equation for the lower medium. For the transmitted wave,

$$x' = s_x\left(\frac{z_1 s_{zR}}{|s_z|^2} + \frac{z_2' s_{zR}'}{|s_z'|^2}\right), \tag{31}$$

where s_x and the quantity between parenthesis are real. It must be solved iteratively for s_x, the stationary value of the horizontal slowness for the incoming and transmitted wave. By using a real value for s_x in eq. (31), we get a corresponding value for x' directly. This may be used in a shooting method to compute s_x when x' is given, but it may also be used to compute results for many values of x' along a receiver line. Although, strictly, a trial-and-error shooting method is not needed, since given x', it should be possible to solve eq. (31) for s_x using the Newton–Raphson method (see Hearn & Krebes 1990). We note that the steepest-descent solution in eq. (13) cannot be used in the same way, as a complex value of the horizontal slowness may not necessarily result in a real value for x'.

For the reflected wave, the stationarity condition gives

$$x = \frac{s_x s_{zR}}{|s_z|^2} z \tag{32}$$

or

$$\left(\frac{z}{x}\right) s_x = s_{zR}\left[1 + \left(\frac{s_{zI}}{s_{zR}}\right)^2\right]. \tag{33}$$

This is a non-linear equation which must be solved for the stationary value s_x (see Appendix B). For small attenuation (s_{zI} small) we obtain the approximations

$$s_x = \frac{x}{r}\sqrt{\mathrm{Re}\left(\frac{1}{v^2}\right)} \tag{34}$$

and

$$s_{zR} = \frac{z}{r}\sqrt{\mathrm{Re}\left(\frac{1}{v^2}\right)}. \tag{35}$$

Compare with eq. (15). For $Q \gg 1$, eq. (34) is the same as eq. (40) in Krebes & Daley (2007).

The stationary phase-approximation of the integral (28) is (Bleistein 1984),

$$u = \frac{A}{4\pi\mu}\frac{F(\tilde{s}_x)}{s_z(\tilde{s}_x)}\left|\frac{2\pi}{\omega\tau_R''(\tilde{s}_x)}\right|^{1/2}\exp[\mathrm{i}\omega\tau_R(\tilde{s}_x) - \omega\tau_I(\tilde{s}_x)]$$
$$\times \exp\left[\mathrm{i}(\pi/4)\mathrm{sgn}\tau_R''(\tilde{s}_x)\right], \tag{36}$$

where all quantities are to be evaluated at the stationary value $s_x = \tilde{s}_x$ computed above. We have, see eq. (8),

$$\tau_I = \begin{cases} z s_{zI}, & \text{for reflection} \\ z_1 s_{zI} + z_2' s_{zI}', & \text{for transmission} \end{cases} \tag{37}$$

and

$$\tau_R'' = \frac{\partial^2 \tau_R}{\partial s_x^2} = \begin{cases} z\dfrac{\partial^2 s_{zR}}{\partial s_x^2}, & \text{for reflection} \\ z_1\dfrac{\partial^2 s_{zR}}{\partial s_x^2} + z_2'\dfrac{\partial^2 s_{zR}'}{\partial s_x^2}, & \text{for transmission,} \end{cases} \tag{38}$$

From eq. (30) we obtain

$$\frac{\partial^2 s_{zR}}{\partial s_x^2} = -\frac{s_{zR}}{|s_z|^2} + \frac{s_x^2 s_{zR}}{|s_z|^6}\left[3s_{zI}^2 - s_{zR}^2\right]. \tag{39}$$

There is a similar equation for the lower medium.

6 GEOMETRICAL RAYS

For the steepest-descent approximation of the transmitted wave (s_x complex), we can write $x' = x_1 + x_2'$ with

$$x_1 = -z_1\frac{\partial s_z}{\partial s_x} = z_1\frac{s_x}{s_z},$$
$$x_2' = -z_2'\frac{\partial s_z'}{\partial s_x} = z_2'\frac{s_x}{s_z'}. \tag{40}$$

Note that, in general, both x_1 and x_2' are complex. But their sum is real, equal to the horizontal distance between the source and receiver.

The complex traveltime is $\tau = \tau_1 + \tau_2'$, with

$$\tau_1 = s_x x_1 + s_z z_1 = \frac{z_1}{s_z v^2},$$
$$\tau_2' = s_x x_2' + s_z' z_2' = \frac{z_2'}{s_z' v'^2}. \tag{41}$$

The complex ray velocities in the upper medium are

$$V_{1x} = \frac{x_1}{\tau_1} = s_x v^2,$$
$$V_{1z} = \frac{z_1}{\tau_1} = s_z v^2, \tag{42}$$

and similar expressions for the ray velocities in the lower medium.

For the stationary-phase approximation (s_x real) of the transmitted wave, we have $x' = x_1 + x_2'$, with

$$x_1 = z_1\frac{s_x s_{zR}}{|s_z|^2},$$
$$x_2' = z_2'\frac{s_x s_{zR}'}{|s_z'|^2} \tag{43}$$

and the traveltime is $\tau = \tau_1 + \tau_2'$ with

$$\tau_1 = s_x x_1 + s_{zR} z_1 = z_1 s_{zR}\left(1 + \frac{s_x^2}{|s_z|^2}\right),$$
$$\tau_2' = s_x x_2' + s_{zR}' z_2' = z_2' s_{zR}'\left(1 + \frac{s_x^2}{|s_z'|^2}\right). \tag{44}$$

This gives the real ray velocities in the upper medium

$$V_{1x} = \frac{x_1}{\tau_1} = \frac{s_x}{s_x^2 + |s_z|^2},$$
$$V_{1z} = \frac{z_1}{\tau_1} = \frac{|s_z|^2}{s_{zR}(s_x^2 + |s_z|^2)}, \tag{45}$$

and similar expressions for the ray velocities in the lower medium.

Using eq. (3) and defining $a \equiv s_z^2$ (see Appendix A), we have for the reflected wave

$$a_R = \frac{1}{v_0^2}\cdot\frac{1}{1+Q^{-2}} - s_x^2$$
$$a_I = \frac{1}{v_0^2}\cdot\frac{1}{Q+Q^{-1}}. \tag{46}$$

For large values of Q (weak loss), we obtain (Appendix A)

$$s_{zR} \approx \sqrt{a_R} \approx \sqrt{\frac{1}{v_0^2} - s_x^2} = \frac{\cos\theta}{v_0}$$
$$s_{zI} \approx \frac{a_I}{2\sqrt{a_R}} \approx \frac{1}{2Qv_0^2\sqrt{v_0^{-2} - s_x^2}} = \frac{1}{2v_0 Q\cos\theta}, \tag{47}$$

where $s_x = \sin\theta/v_0$.

With these simple expressions, the stationary-phase approximation is

$$\exp[\mathrm{i}\omega(s_x x + s_z z)] = \exp\left[\mathrm{i}\omega\left(x\frac{\sin\theta}{v_0} + z\frac{\cos\theta}{v_0}\right)\right]$$
$$\times \exp\left(-\omega\frac{r}{2v_0 Q}\right). \tag{48}$$

This solution corresponds to a ray tracing with a real velocity and computing the attenuation along the ray. Eq. (48) is similar to eqs (36)–(38) of Krebes & Daley (2007). Ray-tracing in anelastic media may break down, even for a homogeneous wave with parallel real

Table 1. Stationary slowness and traveltime of the reflected wave.

Q	s_x^{-1} (m s^{-1})	$\bar{s}_x^{-1}$ (m s^{-1})	s_z^{-1} (m s^{-1})	$\bar{s}_z^{-1}$ (m s^{-1})	τ_R (ms)	$\bar{\tau}_R$ (ms)
∞	3710	3710	2375	2375	74.2	74.2
5	3706	(3729, −369)	(2371, −333)	(2386, −236)	73.3	73.1
1	3500	(4076, −1688)	(2240, −1594)	(2609, −1081)	59.9	57.6

Table 2. Reflection coefficient and damping factor of the reflected wave.

Q	$\|R\|$	$\|\bar{R}\|$	D	$\bar{D}$
∞	0.07	0.07	0.07	0.07
5	0.07	0.1	7.2×10^{-3}	1.1×10^{-2}
1	0.12	0.19	3.2×10^{-5}	1.1×10^{-4}

and complex slowness vectors as it hits an interface, see Krebes & Daley (2007). Vavryčuk (2008) proposes an approximate solution. Our approach in this paper is for plane-wave expansions, and it cannot be expanded to ray-tracing.

7 RESULTS

The reflection and transmission coefficients for *SH* waves in isotropic media are given in eq. (9). For the reflected wave, we have to find its stationary slowness and then compute s_z using eq. (1). In the case of a complex s_x obtained from eq. (15) (the steepest-descent method), s_z and s_z' are given by equations (16) and (17), respectively. For a real s_x (stationary-phase solution), we solve eq. (29) and use eq. (1) and its primed version. For the transmitted wave, we have to find its stationary slowness from equations (13) (steepest-descent solution) and (31) (stationary-phase solution), and s_z and s_z' are given by eq. (1) and its primed version.

7.1 Low-Q comparisons

To compare both approaches, let us consider a specific example, where $x = 80$ m, $z_1 = 70$ m , $x' = 60$ m, $z_2 = 55$ m, $z_2' = 65$ m, and

$$v^2 = 4\left(1 - \frac{\mathrm{i}}{Q}\right) \quad \text{and} \quad v'^2 = 9\left(1 - \frac{\mathrm{i}}{Q'}\right),$$

in [km s^{-1}]^2, so that $v_0 = 2$ km s^{-1} and $v_0' = 3$ km s^{-1}; moreover, $\rho = 2$ g cm^{-3} and $\rho' = 2.2$ g cm^{-3}. The frequency is $f = 50$ Hz and $\omega = 2\pi f$.

We must solve eq. (33) for s_x for the reflected wave and eq. (31) for the transmitted wave, using the results from Appendix A. We solve the equations by stepwise iteration, using the downhill method (Bach 1969a,b). The results for the reflected wave are shown in Tables 1 and 2 for different values of Q and a lossless lower medium (note that eq. 27 is satisfied). The barred symbols correspond to the method of steepest descent, that is, to eq. (15). The positive sign is chosen for all the vertical slowness components, that is, the principal value. The amplitude decay or damping factor from source to receiver is obtained as

$$D = |R \exp[\mathrm{i}\omega(s_x x + s_z z)]| = |R| \exp[-\omega(s_{xI} x + s_{zI} z)],$$

where $s_{xI} = 0$ in the case of the stationary-phase solution (geometrical spreading is not considered).

The initial guess for the transmission problem (eq. 31) is obtained from the lossless case. It can easily be shown that Snell law and $x_1 + x_2' = x'$ lead to a quartic equation in x_1:

$$\begin{aligned} &a_4 x_1^4 + a_3 x_1^3 + a_2 x_1^2 + a_1 x_1 + a_0 = 0, \\ &a_0 = -x'^2 z_1^2 v^2, \\ &a_1 = 2x' z_1^2 v^2, \\ &a_2 = \left(x'^2 + z_2'^2\right) v'^2 - \left(x'^2 + z_1^2\right) v^2, \\ &a_3 = 2x' \left(v^2 - v'^2\right), \\ &a_4 = v'^2 - v^2. \end{aligned} \tag{49}$$

We solve this equation using radicals by Ludovico Ferrari method and obtain $x_1 = 23.9$ m, $s_x^{-1} = 6183$ s m^{-1}, and a traveltime $\tau = 61.8$ ms. The amplitude decay or damping factor from source to receiver is obtained as

$$\begin{aligned} D &= \left|T \exp[\mathrm{i}\omega(s_x x' + s_z z_1 + s_z' z_2')]\right| \\ &= |T| \exp[-\omega(s_{xI} x' + s_{zI} z_1 + s_{zI}' z_2')], \end{aligned}$$

where $s_{xI} = 0$ in the case of the stationary-phase solution.

The results for the transmitted wave are shown in Tables 3 and 4 for different values of Q'. The barred symbols correspond to the method of steepest descent, that is, to eq. (13). An anomalous behaviour is observed in the last case for the steepest-descent case,

Table 4. Traveltime, transmission coefficient and damping factor of the transmitted wave.

Q	Q'	τ_R	$\bar{\tau}_R$	$\|T\|$	$\|\bar{T}\|$	D	$\bar{D}$
∞	∞	61.8	61.8	0.79	0.79	0.79	0.79
5	∞	61.2	61.2	0.79	0.79	0.26	0.26
5	10	61.2	61.1	0.79	0.79	0.17	0.17
1	∞	53.8	53.6	0.89	0.88	2×10^{-2}	2×10^{-2}
1	10	53.7	53.5	0.89	0.87	1.3×10^{-2}	1.3×10^{-2}
0.7	1	45	31	0.83	1.17	1.5×10^{-3}	0.26

Table 3. Stationary slowness and traveltime of the transmitted wave.

Q	Q'	s_x^{-1} (m s^{-1})	$\bar{s}_x^{-1}$ (m s^{-1})	s_z^{-1} (m s^{-1})	$\bar{s}_z^{-1}$ (m s^{-1})	$s_z'^{-1}$ (m s^{-1})	$(\bar{s}_z')^{-1}$ (m s^{-1})
∞	∞	6183	6183	2114	2114	3431	3431
5	∞	6190	(6190, −223)	(2121, −235)	(2123, −226)	(3430, 0)	(3427, +38)
5	10	6190	(6198, −420)	(2121, −235)	(2124, −218)	(3430, −224)	(3433, −152)
1	∞	6321	(6332, −1063)	(2253, −1083)	(2310, −1050)	(3408, 0)	(3357, +150)
1	10	6321	(6354, −1255)	(2253, −1083)	(2316, −1041)	(3409, −220)	(3371, −37)
0.7	1	6442	(2486, −752)	(2347, −1457)	(1493, −4026)	(3419, −1993)	(688, +3642)

when considering diffusion-like Q values. Note that the real horizontal slowness component is not equal to the real part of the complex slowness components obtained with the steepest-descent method (they are equal for $Q \gg 1$).

7.2 Comparison of reflection and transmission coefficients

7.2.1 Reflection coefficient

Let us consider now a similar problem studied by Krebes and Daley illustrated in their figs 1–10 (Krebes & Daley 2007). Here, we assume a Maxwell mechanical model to describe the anelasticity, whose complex velocity is

$$v = v_0\sqrt{\frac{Q}{Q - \mathrm{i}(\omega_0/\omega)}},$$

and its primed version (e.g. Carcione 2014), where ω_0 is a reference frequency, with $v_0 = 1$ km s^{-1}, $v_0' = 2$ km s^{-1}, $Q = 15$, $Q' = 20$, $\rho = 2$ g cm^{-3} and $\rho' = 2.1$ g cm^{-3} (Q is the quality factor at ω_0). The frequency-dependent quality factor is $\omega\eta/(\rho v_0^2)$, where the Maxwell viscosity $\eta = \rho v_0^2 Q/\omega_0$. Krebes & Daley (2007) show that choosing the sign of the vertical slowness component to satisfy the radiation condition ($\mathrm{Im}(s_z') > 0$), the transmitted wave amplitude decays with distance away from the interface) involves large errors in the absolute value of the reflection coefficient. On the other hand, choosing the principal value (a Fortran compiler yields this value) implies large discrepancies in the phase and the anelastic reflection coefficient does not tend to the elastic one as the anelasticity is decreased. In their second approach they take a real horizontal slowness components as the real part of the steepest-descent solution, which is not the same as the solution obtained from eq. (29). The solution of Krebes & Daley (2007) only agree approximately for $Q \gg 1$ with our solution that applies for very low Q as well. For $Q \gg 1$, s_x is approximately the real part of the steepest descent s_x. In addition, we consider a receiver in the lower medium (the transmission problem) and check our results with numerical simulations (see below).

Fig. 2 shows the reflection coefficient obtained with steepest-descent method (dashed line) and stationary-phase method (solid line). The dotted line corresponds to the lossless case. While the absolute values of the reflection coefficient are similar, the phases are

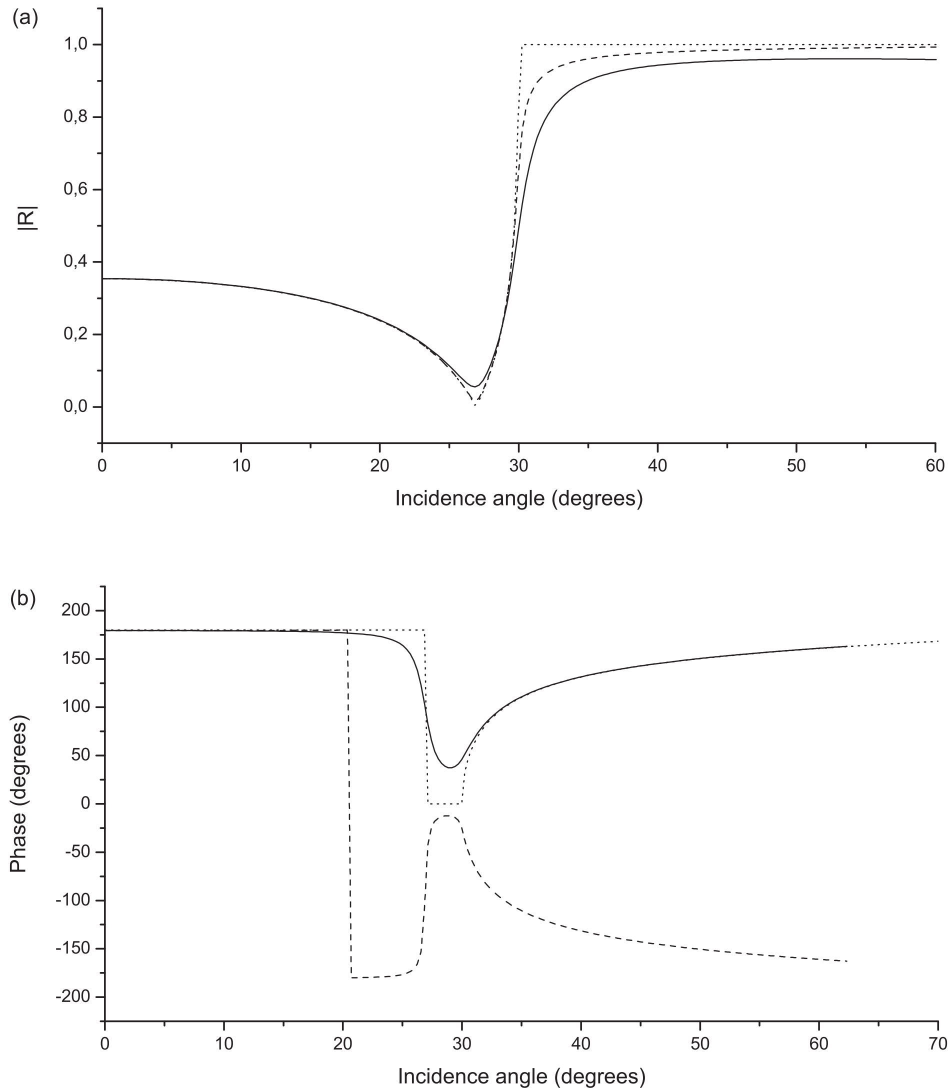

Figure 2. Reflection coefficient for the lossless, stationary-phase and steepest-descent cases (dotted, solid and dashed lines, respectively). Square roots in the second case are computed as the principal value.

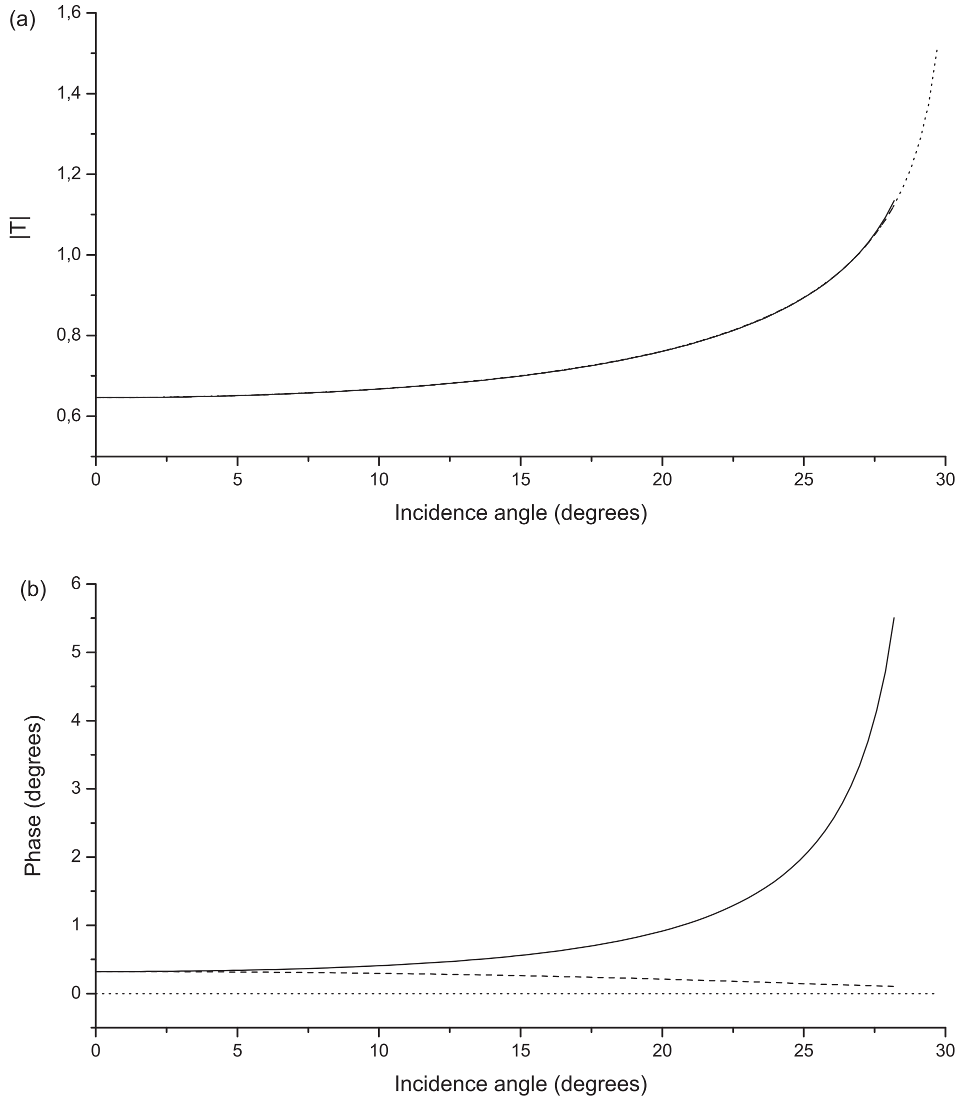

Figure 3. Transmission coefficient for the lossless, stationary-phase and steepest-descent cases (dotted, solid and dashed lines, respectively). Square roots in the second case are computed as the principal value.

very different, indicating problems when the stationary slowness is complex (steepest-descent method). The results for a real horizontal slowness are similar to those of the lossless case as should be expected.

7.2.2 Transmission coefficient

To obtain the initial guess for the transmission problem, we assume the incidence angle θ, calculate $x_1 = z_1 \tan\theta$ and find the location of the receiver x'. From equation (49), we obtain

$$
\begin{aligned}
&b_2 x'^2 + b_1 x' + b_0 = 0,\\
&b_0 = (v'^2 - v^2)x_1^4 + x_1^2({z_2'}^2 v'^2 - z_1^2 v^2),\\
&b_1 = 2z_1^2 v^2 x_1 - 2(v'^2 - v^2)x_1^3,\\
&b_2 = x_1^2(v'^2 - v^2) - z_1^2 v^2. \qquad (50)
\end{aligned}
$$

The solution is $x' = -(b_1 + \sqrt{b_1^2 - 4b_0 b_2})/(2b_2)$ and can be obtained up to the critical angle $\theta_C = \sin^{-1}(v'/v)$, since beyond this angle $x' = \infty$, with $x_{1C} = z_1 \tan\theta_C$.

Fig. 3 shows the transmission coefficient obtained with steepest-descent method (dashed line) and stationary-phase method (solid line). The dotted line corresponds to the lossless case. There is no noticeable difference between the different coefficients below the elastic critical angle. As we show below, the difference appears after that angle. In this case, the phase corresponding to the steepest-descent method is closer to the elastic phase, although the differences are small, of the order of a few degrees. The numerical evaluation of the transmission coefficient below shows that the stationary-phase solution is the correct one and represents a conclusive test.

7.3 Numerical test

We use the method outlined in Appendix C to obtain the reflection and transmission coefficients. Two meshes with 243 × 81 grid points model the interface, with a grid size $dx = 10$ m and a vertical extent of 510 m for each mesh. To avoid unphysical reflections from the sides, top of the upper mesh and bottom of the lower mesh, we use absorbing boundaries of 40 and 18 grid points width. In addition, non-reflecting boundary condition is implemented along the vertical

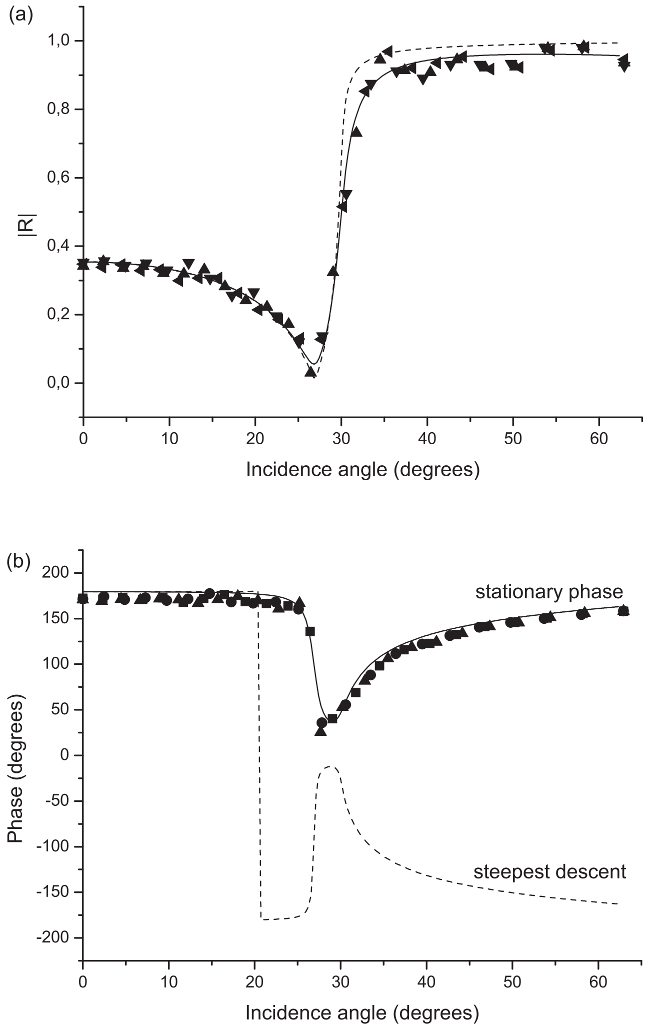

Figure 4. Reflection coefficient (a) and phase angle (b) as a function of the angle of incidence. The solid and dashed lines correspond to the stationary-phase and steepest-descent solutions, respectively. The symbols indicate the numerical evaluation for different frequencies (9 (triangles), 10 (circles) and 11 (squares) Hz).

direction. The source, located 212 m above the interface, is a Ricker wavelet with a dominant frequency of 10 Hz. We propagate the wavefield with a time step of 1 ms.

Figs 4 and 5 show the comparison between the analytical and numerical solutions. The solid and dashed lines correspond to the stationary-phase and steepest-descent solutions, while the symbols indicate the numerical evaluation for different frequencies. As can be seen, the correct physical solution is that of the stationary-phase method with a real horizontal slowness. The analytical transmission coefficients in Fig. 5 are computed with the stationary slowness of the reflected wave. Although this is an approximation, the results indicate that the stationary-phase solution is the one which is in better agreement with the numerical evaluation.

8 CONCLUSIONS

Reflected and transmitted *SH* waves from an interface between two homogeneous anelastic half spaces can be exactly computed by an integral over frequency and real horizontal slowness. The steepest-descent approximation gives a stationary value for the horizontal slowness that is complex and horizontal distances which are complex. In some cases, the dispersion relation gives complex vertical slownesses for up- and down-going waves which both have increasing amplitude in the direction of wave propagation. Both the complex horizontal distances and the exponentially increasing wave amplitudes are non-physical effects. The stationary-phase approximation to the slowness integral gives real horizontal slownesses and real horizontal distances. This is a physical wave solution which will not violate the radiation condition. The amplitude always decreases in the direction of wave propagation.

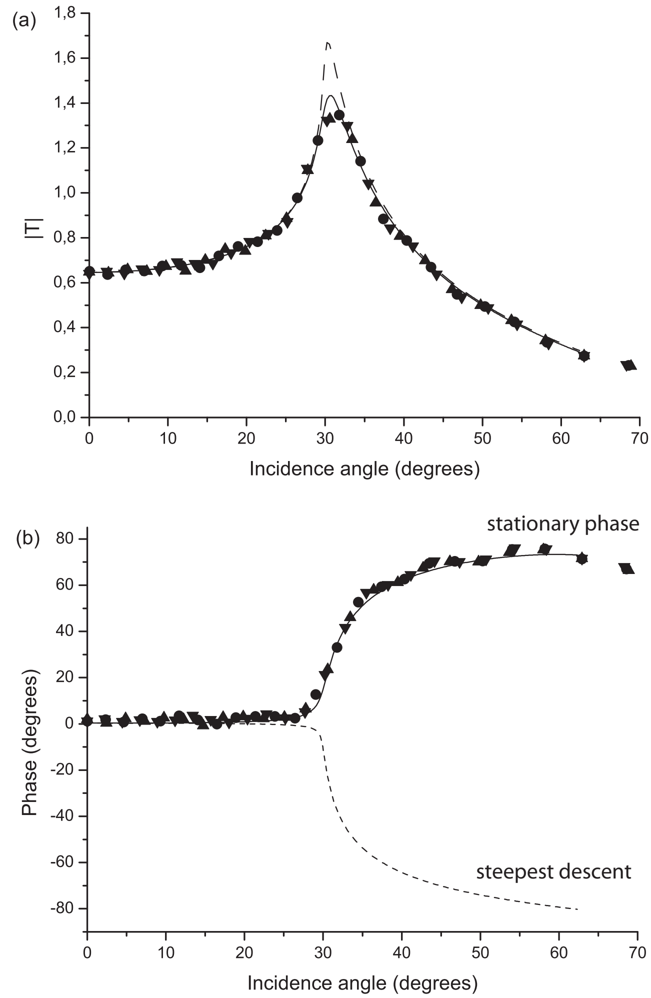

Figure 5. Transmission coefficient (a) and phase angle (b) as a function of the angle of incidence. The solid and dashed lines correspond to the stationary-phase and steepest-descent solutions, respectively. The symbols indicate the numerical evaluation for different frequencies (9 (triangles up), 10 (circles) and 11 (triangles down) Hz).

Moreover, by using a real value for horizontal slowness, we get a corresponding value for the horizontal distance, which may be used to compute results along a receiver line, while the steepest-descent solution cannot be used in the same way, as a complex value of the horizontal slowness may not necessarily result in a real value for the distance. The results are compared to numerical simulations indicating that the stationary-phase solution with a real horizontal slowness is the correct solution.

By virtue of mathematical analogies, the theory developed here can be applied to sound and electromagnetic waves. The generalization to the anisotropic case (for *SH* and *P–SV* waves) is straightforward and will be performed in a future work as well as the implications on Fermat principle.

ACKNOWLEDGEMENTS

BU has received financial support from Statoil, Brazil, from CNPq, Brazil and from the Norwegian Research Council through the ROSE project. We thank Edward Krebes for his detailed review. We also thank Roger Borcherdt for his comments.

REFERENCES

Aki, K. & Richards, P.G., 2002. *Quantitative Seismology,* 2nd edn, University Science Books.

Bach, H., 1969a. On the downhill method, *Commun. ACM,* **12,** 675–678.

Bach, H., 1969b. Algorithm 365: complex root finding, *Commun. ACM,* **12,** 686–687.

Bleistein, N., 1984. *Mathematical Methods for Wave Phenomena,* Academic Press.

Borcherdt, R.D., 1977. Reflection and refraction of type-II S waves in elastic and anelastic media, *Bull. seism. Soc. Am.,* **67,** 43–67.

Borcherdt, R.D., 2009. *Viscoelastic Waves in Layered Media,* Cambridge Univ. Press.

Borcherdt, R.D. & Wennerberg, L., 1985. General P, type-I S, and type-II S waves in anelastic solids: inhomogeneous wave fields in low-loss solids, *Bull. seism. Soc. Am.,* **75,** 1729–1763.

Borcherdt, R.D., Glassmoyer, G. & Wennerberg, L., 1986. Influence of welded boundaries in anelastic media on energy flow, and characteristics of P, S-I, and S-II waves: observational evidence for inhomogeneous body waves in low-loss solids, *J. geophys. Res.,* **91,** 11 503–11 518.

Brokešová, J. & Červený, V., 2002. Viscoelastic R/T problem for arbitrary orientation of propagation and attenuation vectors, in *64th EAGE Conference & Exhibition,* Florence, Italy.

Carcione, J.M., 1999. On energy definition in electromagnetism: an analogy with viscoelasticity, *J. acoust. Soc. Am.,* **105**(2), 626–632.

Carcione, J.M., 2014. Wave fields in real media: wave propagation in anisotropic, anelastic, porous and electromagnetic media, in *Handbook of Geophysical Exploration,* 3rd edn, revised and extended, Elsevier.

Carcione, J.M. & Helle, H.B., 2004. On the physics and simulation of wave propagation at the ocean bottom, *Geophysics,* **69,** 825–839.

Carcione, J.M. & Robinson, E., 2002. On the acoustic-electromagnetic analogy for the reflection-refraction problem, *Stud. Geophys. Geod.,* **46,** 321–345.

Carcione, J.M. & Ursin, B., 2016. On Fermat principle and Snell law in lossy anisotropic media, *Geophysics,* **3,** T107–T116.

Carcione, J.M., Gei, D., Botelho, M.A.B., Osella, A. & de la Vega, M., 2006. Fresnel reflection coefficients for GPR-AVO analysis and detection of seawater and NAPL contaminants, *Near Surf. Geophys.,* **4,** 253–263.

Chapman, C.H., 2004. *Fundamentals of Seismic Wave Propagation,* Cambridge Univ. Press.

Daley, P.F. & Krebes, E.S., 2004. SH wave propagation in viscoelastic media, *Stud. Geophys. Geod.,* **48,** 563–587.

Daley, P.F. & Krebes, E.S., 2015. Anelastic (poroviscoelastic) medium - the SH-wave problem, *J. Seismol. Explr.,* **24,** 103–120.

Hearn, D.J. & Krebes, E.S., 1990. On computing ray-synthetic seismograms for anelastic media using complex rays, *Geophysics,* **55,** 422–432.

Krebes, E.S. & Daley, P.F., 2007. Difficulties with computing anelastic plane-wave reflection and transmission coefficients, *Geophys. J. Int.,* **170,** 205–216.

Krebes, E.S. & Slawinski, M.A., 1991. On raytracing in an elastic-anelastic medium, *Bull. seism. Soc. Am.,* **81,** 667–686.

Richards, P.G., 1984. On wave fronts and interfaces in anelastic media, *Bull. seism. Soc. Am.,* **74,** 2157–2165.

Ruud, B.O., 2006. Ambiguous reflection coefficients for anelastic media, *Stud. Geophys. Geod.,* **50,** 479–498.

Sidler, R., Carcione, J.M. & Holliger, K., 2008. On the evaluation of the plane-wave reflection coefficients in anelastic media, *Geophys. J. Int.,* **175,** 94–102.

Tsvankin, I., 1995. *Seismic Wavefields in Layered Isotropic Media,* Samizdat Press. Available at: http://samizdat.mines.edu/wave_layered_media/.

Ursin, B. & Stovas, A., 2002. Reflection and transmission responses of a layered isotropic viscoelastic medium, *Geophysics,* **67,** 307–323.

Vavryčuk, V., 2008. Real ray tracing in anisotropic viscoelastic media, *Geophys. J. Int.,* **175,** 617–626.

Vavryčuk, V., 2010. Behaviour of rays at interfaces in anisotropic viscoelastic media, *Geophys. J. Int.,* **181,** 165–1677.

APPENDIX A: THE VERTICAL SLOWNESS

The dispersion relation (1) can be expressed by

$$s_z^2 = s_{zR}^2 - s_{zI}^2 + 2\mathrm{i}s_{zR}s_{zI} = a_R + \mathrm{i}a_I = a, \tag{A1}$$

where

$$a = \frac{1}{v^2} - s_x^2$$

for the steepest-descent method (s_x complex) and the stationary-phase method (s_x real).

From eq. (A1) we obtain

$$s_{zI} = \frac{a_I}{2s_{zR}}. \tag{A2}$$

When this is used in eq. (A1), we obtain a second-order equation for s_{zR}. We choose the positive solution, giving

$$s_{zR}^2 = \frac{1}{2}(a_R + |a|). \tag{A3}$$

From eq. (A1) or from eqs (A2) and (A3) we obtain

$$|s_z|^2 = s_{zR}^2 + s_{zI}^2 = |a|$$

$$= \sqrt{\left[\mathrm{Re}\left(\frac{1}{v^2} - s_x^2\right)\right]^2 + \left[\mathrm{Im}\left(\frac{1}{v^2} - s_x^2\right)\right]^2}. \tag{A4}$$

From eq. (4), with real s_x,

$$a_R = \frac{1}{v_0^2}\frac{1}{1+1/Q^2} - s_x^2 \tag{A5}$$

and

$$\frac{a_I}{a_R} = \left\{Q\left[1 - v_0^2\left(1 + \frac{1}{Q^2}\right)s_x^2\right]\right\}^{-1}. \tag{A6}$$

Eq. (A3) has two solutions for s_{zR}, a positive solution for downgoing waves and a negative solution for upgoing waves. But for the reflected wave the difference in vertical coordinates is also negative, resulting in eq. (29) with positive s_{zR}.

In the lossless case, $Q \to \infty$, so that $A = 2$, $a_I = 0$ and $s_{zR} = \sqrt{a_R}$ and eq. (29) can be solved analytically, giving

$$s_x = \frac{x}{v_0 r} = \frac{\sin\theta}{v_0}. \tag{A7}$$

The reflection traveltime is

$$\tau = \frac{x}{v_0 \sin\theta}, \tag{A8}$$

as can be deduced from simple geometrical arguments.

APPENDIX B: THE STATIONARY-PHASE SOLUTION FOR THE HORIZONTAL SLOWNESS

For the reflected wave the stationary-phase solution is given in eq. (33) which becomes

$$s_x^2 = \left(\frac{x}{z}\right)^2 \left(s_{zR}^2 + 2s_{zI}^2 + \frac{s_{zI}^4}{s_{zR}^2}\right) = \mathrm{Re}\left(\frac{1}{v^2}\right) - s_{zR}^2 + s_{zI}^2, \quad \text{(B1)}$$

where we have used the dispersion relation (A1) for s_x real. With eq. (A2) this gives

$$\mathrm{Re}\left(\frac{1}{v^2}\right) = \left(\frac{r}{z}\right)^2 s_{zR}^2 + \frac{1}{4s_{zR}^2}\left[2\left(\frac{x}{z}\right)^2 - 1\right] \times \left[\mathrm{Im}\left(\frac{1}{v^2}\right)\right]^2 + \frac{1}{16s_{zR}^6}\left(\frac{x}{z}\right)^2\left[\mathrm{Im}\left(\frac{1}{v^2}\right)\right]^4. \quad \text{(B2)}$$

Neglecting the last term, we obtain a second-order equation for s_{zR}^2. The result is

$$s_{zR}^2 = \frac{1}{2}\left(\frac{z}{r}\right)^2 \left\{\mathrm{Re}\left(\frac{1}{v^2}\right) + \sqrt{\left|\frac{1}{v^2}\right| - 2\left(\frac{x}{z}\right)^2 \left[\mathrm{Im}\left(\frac{1}{v^2}\right)\right]^2}\right\}, \quad \text{(B3)}$$

so that

$$s_{zR}^2 = \left(\frac{z}{r}\right)^2 \left\{\frac{1}{2}\mathrm{Re}\left(\frac{1}{v^2}\right) \times \left[1 + \sqrt{1 + \left[1 - 2\left(\frac{x}{z}\right)^2\right]\left[\mathrm{Im}\left(\frac{1}{v^2}\right)/\mathrm{Re}\left(\frac{1}{v^2}\right)\right]^2}\right]\right\}, \quad \text{(B4)}$$

From this value of s_{zR} we obtain

$$s_{zI} = \frac{1}{2s_{zR}}\mathrm{Im}\left(\frac{1}{v^2}\right) \quad \text{(B5)}$$

and then from eq. (32),

$$s_x = s_{zR}\left(\frac{x}{z}\right)\left[1 + \frac{1}{4s_{zR}^4}\mathrm{Im}\left(\frac{1}{v^2}\right)^2\right]. \quad \text{(B6)}$$

We see that eqs (B4) and (B6) reduce to eqs (34) and (35) for small attenuation.

APPENDIX C: NUMERICAL EVALUATION OF THE REFLECTION AND TRANSMISSION COEFFICIENTS

Let us consider the *SH*-wave equation of the mechanical Maxwell model in the (x, z)-plane, equivalent to Maxwell's TM wave equation (Carcione & Robinson 2002),

$$\partial_x \sigma_{xy} + \partial_z \sigma_{yz} = \rho \partial_t v_y + s,$$
$$\partial_t \sigma_{yz} = \rho v_0^2 (\partial_z v_y - \eta^{-1}\sigma_{yz}),$$
$$\partial_t \sigma_{xy} = \rho v_0^2 (\partial_x v_y - \eta^{-1}\sigma_{xy}), \quad \text{(C1)}$$

where v_y is the particle velocity, σ denotes stress, s is a source and ∂ indicates partial derivative (e.g. Carcione 2014).

In order to obtain the reflection and transmission coefficients from space–time domain data, we compute synthetic seismograms by using a domain-decomposition method to model the upper and lower media by using two grids (Carcione *et al.* 2006) and the equation of motion for shear waves. The spatial derivatives are computed with the Fourier and Chebyshev pseudospectral methods along the horizontal and vertical direction, respectively, and a fourth-order Runge–Kutta algorithm is used a time solver. This method has been applied with success to obtain the reflection coefficient of the ocean bottom in the presence of the viscoelastic Rayleigh-window phenomenon (Carcione & Helle 2004).

The inversion method for the reflection coefficient consists on the following:

(1) Generate a synthetic seismogram of the particle velocity v_y (propagation in the (x, y)-plane), placing a line of receivers at the penultimate row of grid points above the interface. This seismogram contains the incident and reflected fields.

(2) Compute the synthetic seismogram without interface (the lower medium is set equal to the upper medium) at the same location. This seismogram contains the incident field only.

(3) Perform the difference between the first and second seismograms. The difference contains the reflected field only.

(4) Perform an (ω, k_x)-transform of the incident field to obtain $v_{y0}(\omega, k_x)$, where ω is the angular frequency and k_x is the horizontal wavenumber.

(5) Perform an (ω, k_x)-transform of the reflected field to obtain $v_y(\omega, k_x)$.

(6) Define $A = v_y(\omega, k_x)/v_{y0}(\omega, k_x)$; the quantity $|A|$ is the absolute value of the reflection coefficient, and the phase angle is given by $\tan^{-1}[\mathrm{Im}(A)/\mathrm{Re}(A)]$. Then, transform k_x to incidence angle by using $\sin\theta = v_p k_x/\omega$, where v_p is the phase velocity in the upper medium at the reference frequency ω_0 ($v_p = 1/\mathrm{Re}[1/v(\omega_0)]$) (Carcione 2014).

Regarding the transmission coefficient, generate a synthetic seismogram of the particle velocity v_y placing a line of receivers at the second row of grid points below the interface. This seismogram contains the transmitted wave field. Then, compute the synthetic seismogram without interface (the lower medium is set equal to the upper medium) at the same location. This seismogram contains the incident field only. Then, proceed with points 4 to 6 above.